Journal of Plastic, Reconstructive & Aesthetic Surgery (2019) 72, 572–580

JPRAS
An International Journal of Surgical Reconstruction
www.JPRASurg.com

Navigation-guided fibula free flap for mandibular reconstruction: A proof of concept study

Piotr Pietruski[a,b,*], **Marcin Majak**[c], **Ewelina Światek-Najwer**[c], **Magdalena Żuk**[c], **Michał Popek**[c], **Maciej Mazurek**[a], **Marta Świecka**[a], **Janusz Jaworowski**[a]

[a] *Department of Applied Pharmacy and Bioengineering, Medical University of Warsaw, Banacha 1 Street, 02-097 Warsaw, Poland*
[b] *Department of Plastic Surgery, Prof. W. Orlowski Memorial Hospital, Medical Centre of Postgraduate Education, Czerniakowska 231 Street, 00-416 Warsaw, Poland*
[c] *Faculty of Mechanical Engineering, Wroclaw University of Science and Technology, Lukasiewicza 7/9 Street, 50-370 Wroclaw, Poland*

Received 23 August 2018; accepted 18 January 2019

KEYWORDS
Mandible reconstruction;
Free fibula flap;
Image-guided surgery;
Computer-assisted surgery;
Intraoperative navigation

Summary *Objective:* To analyze a novel technique of supporting fibula free flap harvest and fabrication with intraoperative navigation technology.
Materials and methods: In the first phase of the study, navigation accuracy achieved with two registration methods, namely, point-pair and hybrid technique utilizing point-pair with surface matching, were evaluated in the form of the fiducial (FRE) and target registration error (TRE). Next, a series of 42 simulated navigated fibular osteotomies were conducted on specially manufactured lower leg phantom. Postoperative results were analyzed in the form of the angular and position deviations between the virtually planned and the obtained osteotomies.
Results: Mean FRE values obtained with point-pair and hybrid registration methods were 1.82 ± 0.96 mm and 1.41 ± 0.44 mm, respectively. Mean TRE value in the fibula region was 2.00 ± 0.67 mm for the first method and 1.51 ± 0.72 mm for the second. For all performed surgeries, the total mean angular deviation between the planned and actual osteotomy trajectory equaled 3.66° ± 3.60°. The total mean position disparity of osteotomy control points was 1.85 ± 0.99 mm.
Conclusions: Navigation-guided free fibula flap harvest and fabrication, due to encouraging study results and its superiority over currently popular cutting guides in many clinical aspects,

* Corresponding author at: Department of Plastic Surgery, Prof. W. Orlowski Memorial Hospital, Medical Centre of Postgraduate Education, Czerniakowska 231 Street, 00-416 Warsaw, Poland.
E-mail address: pietruski.piotr@gmail.com (P. Pietruski).

https://doi.org/10.1016/j.bjps.2019.01.026

may become a routine operative procedure for the reconstruction of complex mandibular defects. The presented method is especially well suited for plastic and maxillofacial surgery.

Introduction

Fibula free flap (FFF), first described by Hidalgo in 1988, is currently considered a workhorse of the reconstruction of complex mandibular defects.[1] Many previous studies demonstrated that this method produces satisfactory long-term functional and esthetic outcomes.[2-6] However, the procedure is technically challenging and time-consuming. Restoration of the three-dimensional (3D) structure of the mandible, which is capable of normal occlusion, speech, and mastication, requires accurate positioning and contouring of harvested fibular segments. Unfortunately, conventional shaping, insertion, and fixation of bone fragments are to a large extent dependent on surgeon's experience and, thus, not infrequently, may be imprecise.[7-9]

In recent decades, virtual surgical planning (VSP) and computer-aided design and manufacturing (CAD/CAM) have been recognized as reliable methods to support mandibular reconstruction with FFF.[10-18] Initially, those technologies were used to create stereolithic models of the mandible and fibula based on preoperative CT scans, to be used to simulate the reconstruction procedure and/or serve as an anatomical reference during the proper surgery (Figure 1(A)).[7,13,19] However, the strategy of computer-assisted surgery (CAS) has been evolving over time. Presently, a virtual plan for mandibular resection and reconstruction with an osteocutaneous flap is prepared first, and then, the procedure is conducted with the aid of patient-specific osteotomy guides and prebent plates (Figure 1(B)).[9-18,20-23] Using the CAD/CAM cutting guides, the surgeon can harvest an osseous flap, the optimal characteristics of which, such as localization, size, and angulation, have been previously determined on a virtual model. This facilitates correct positioning and approximation of the fibular segments and creation of the neomandible with desired characteristics.[8,12,13,20-24] Previous studies demonstrated that application of the VSP with CAD/CAM improved the accuracy and efficiency of mandibular reconstruction and contributed to the reduction of operating time and overall treatment cost.[8-11,13,17,24-26]

Intraoperative navigation is another CAS technique gaining a growing popularity among oral and maxillofacial surgeons. This technology, also referred to as image-guided surgery (IGS), facilitates accurate tracking of the pointer or surgical instrument within a 3D surgical field in real time. Using this feature, combined with VSP technology, the surgeon can perform complex procedures in anatomical areas, the dissection of which is technically demanding, such as the head and neck.[27] Intraoperative navigation has been used for the resection of mandibular tumors and reconstruction of the mandible, as well as during other procedures, such as the implantation, temporomandibular joint arthroplasty, and guided biopsy.[27-32] Although this technique is in many aspects superior to VSP and CAD/CAM fusion, the applicability of IGS during FFF harvesting for mandibular reconstruction has been a subject of only one published study.[33]

In this preclinical study, we verified an innovative concept of virtually planned harvesting and fabrication of FFF for the reconstruction of mandibular defect, supported with intraoperative navigation (Figure 1(C)). In our opinion, this method may constitute another step in the evolution of computer-assisted techniques used in plastic and maxillofacial surgery.

Material and methods

Image data acquisition

The specially designed phantom was scanned using a 32-slice CT scanner (Somatom Sensation 16; Siemens Medical Solutions, Erlangen, Germany) (Figure 2). The 512×512 pixel dataset was acquired at a voxel size of 0.39 mm and 0.625 mm slice thickness. The image data were saved in Digital Imaging and Communication in Medicine (DICOM) format and then exported to planning software of the MentorEye system (Wroclaw University of Technology, Wroclaw, Poland).[34] The phantom was also scanned using a 3D Surface scanner (Artec Space Spider, Artec3D, Luxembourg, Luxembourg) with a blue LED light source. Acquired scans were analyzed using Artec Studio Professional 10 to obtain data for further registration processing.

Evaluation of registration accuracy

The reference frame was firmly attached to the anterior border of the tibia using a transcutaneous approach. Two registration methods were evaluated during the study. In the first method, hybrid matching, both 3D images of the phantom's skin surface obtained by CT imaging and an optical scanner were fused with initial alignment acquired with point-pair registration based on 4 surface point-pairs. The second method, referred to as point-pair, was based only on the integration of pairs of corresponding points in the real and virtual operating field. The adhesive skin markers were used as the registration fiducials. During the first stage, 15 configurations with 9 ($n = 5$), 8 ($n = 5$), or 7 ($n = 5$) registration points in different locations were tested. Then, based on the accuracy of each configuration, expressed as a fiducial registration error (FRE), the final point-pair registration method was developed.[35]

After registration, the lateral part of the phantom's skin integument was removed, to expose the skeletal structures. Using the openings drilled on the lateral surface of the fibula as target fiducials, the accuracy of intraoperative navigation, expressed as the target registration error (TRE),

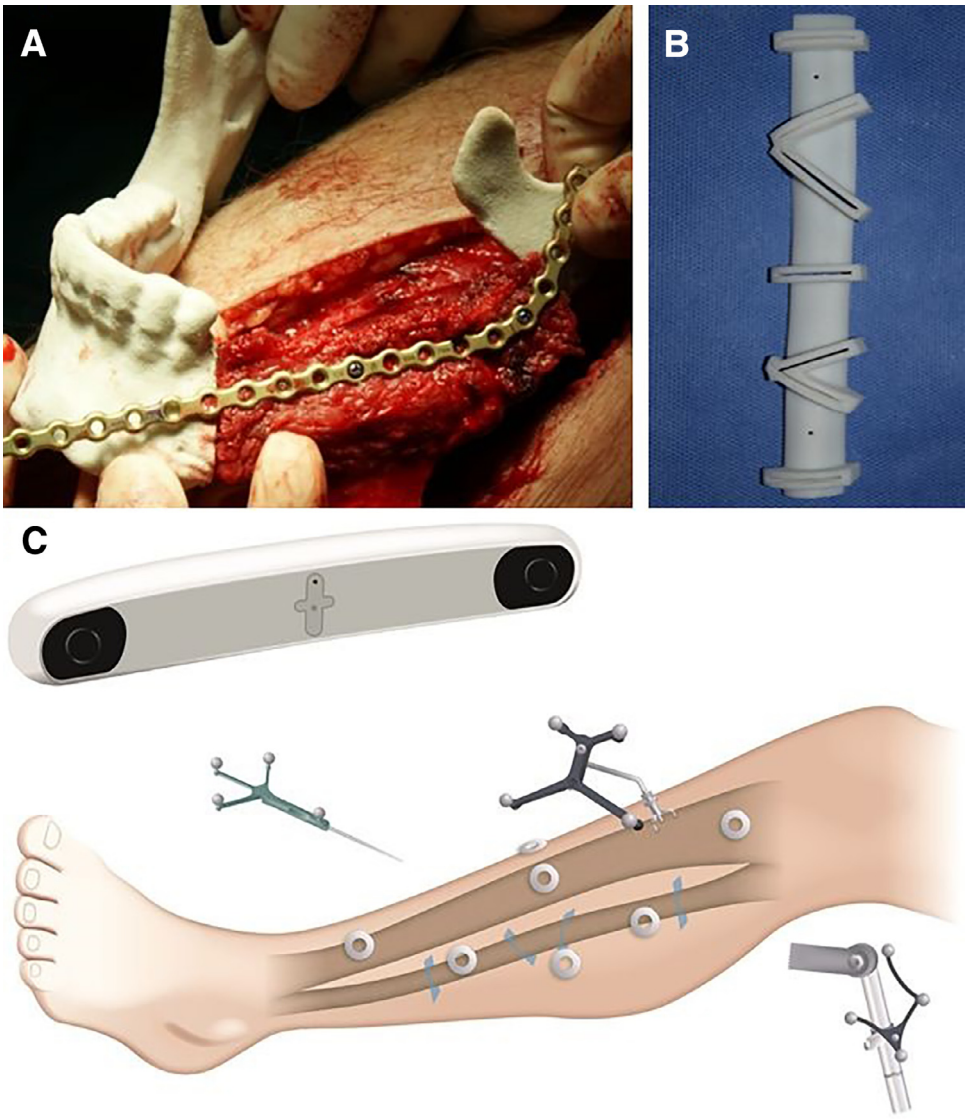

Figure 1 Methods used for computer-assisted mandibular reconstruction with free fibula flap. (A) Contouring of fibular segments based on stereolithic model of the mandible. (B) Patient-specific cutting guide for osteotomy and prefabrication of the fibula in situ. (C) Authors' concept of navigation-guided harvesting of fibula flap. The method is based on minimally invasive transdermal fixation of the reference frame to the anterior border of the tibia, which is then used to track the position of the fibula. The registration points are seven adhesive skin markers placed as shown in the figure. The osteotomy, conducted according to the virtual surgical plan, can be carried out with a navigated pointer or saw.

was determined. TRE was automatically computed by the software as the square root of the sum of squared deviations in all three spatial directions.[35] Registration with each method, along with the determination of TRE, has been performed in three sessions by two researchers independently.

Navigation-guided fibula osteotomies

Using virtual planning module of the MentorEye system, seven osteotomies were designed on the removable fibular segments (Figure 3(A)). The registration was carried out using the point-pair technique with seven skin registration points, as it was shown to be the most accurate in previously described validation test of this method (Figure 1(C)). The registration process was carried out with a pointer. The reference frame was inserted transdermally and screwed securely to the anterior border of the tibia. Then, a sagittal surgical saw (GB129R, Aesculap, Center Valley, PA, USA) was calibrated; hence, the position and angulation of its blade could be displayed in a real time on a screen in multiplanar two-dimensional (2D) cross-sections and 3D views of the operating field. The accuracy of the saw's navigation was verified by placement of the pointer on various anatomical landmarks and comparison of its localization and angulation within physical and virtual space. Then, after removal of the phantom's skin integument, the simulated surgery was conducted according to the virtual plan.

Each of the seven osteotomies were represented by virtual planes in the three-dimensional coordinate system.

Figure 2 Lower leg phantom. The phantom consisted of the tibia, fibula, and foot skeleton covered with a removable outer layer corresponding to the skin integument, all made of gypsum composite. The central segment of the fibula, 20 cm in length, could be dismantled and mantled again. To verify the accuracy of navigation, ten anatomical landmarks in form of 1.2-mm holes were created on the fibular segment. Moreover, 16 adhesive skin markers, serving as registration points, were placed on the outer layer of the phantom.

During the procedure, the saw's blade was navigated against the selected osteotomy plane, and the system displayed the distance and angulation of the blade in relation to the designated osteotomy line as numeric data. This feature, combined with visualization of the saw's position on 2D cross-sections and 3D images, enabled us to perform all seven osteotomies according to the virtual plan (Figure 3(B)). The procedures were conducted on six identical fibular segments mounted in the phantom.

Postoperative evaluation

Postoperative CT scans, with identical imaging parameters, were obtained for all operated fibular segments. Using MentorEye software, postoperative image data in DICOM format were fused with the virtual preoperative CT-based plan, by labeling corresponding fiducial points on the fibula (Supplemental figure). After superimposition of the image data, the following parameters were analyzed twice: angular deviation from each planned osteotomy trajectory and the deviation (calculated using the same formula as for the TRE parameter) in the location of the control points labeled on the edges of the trajectory of the obtained and planned osteotomy.

Statistical analysis

Statistical analysis of the differences between the planned and the obtained osteotomies was performed using one-way analysis of variance (ANOVA) with Tukey post-hoc test. The intra-observer variability between the first and the second evaluation was assessed using the Bland-Altman method. All calculations were carried out with Statistica 10 package (StatSoft, United States), with the threshold of statistical significance set at $p < 0.05$.

Results

Mean FRE values obtained during the preliminary tests of point-pair registration with 9, 8, and 7 registration points were 2.96 ± 0.29 mm, 2.6 ± 0.22 mm, and 2.51 ± 0.34 mm, respectively. With these results, the final protocol of the point-pair registration was developed, with seven registration points placed as shown in Figure 1(C). The data illustrating the accuracy of registration and navigation with this method are presented in Table 1, along with the corresponding data for the surface matching method.

A total of 42 simulated navigated osteotomies were conducted on six identical models of the fibula. Mean FRE value calculated for all procedures was 1.89 ± 0.07 mm. During each osteotomy, the postoperative image data could be successfully fused with the data recorded in the virtual operation plan. The deviations of postoperative outcomes from the assumption of virtual plan are shown in Tables 2 and 3. The differences between the goals of virtual planning and the postoperative results are summarized in Tables 2 and 3. For all performed surgeries, the total mean angular deviation between the planned and actual osteotomy trajectory equaled $3.66° \pm 3.60°$. Overall, the angular deviation of osteotomy C was found to be significantly higher than that in other types of osteotomies, excluding type F ($p = 0.296$) (Table 4). The total mean position disparity of osteotomy control points was 1.85 ± 0.99 mm.

Discussion

Virtual planning with CAD/CAM guides is currently a leading trend in guided mandibular reconstruction with FFF. However, this method is not free from some drawbacks. Its primary limitation is the high cost of designing and creating a cutting template, which, depending on manufacturer and procedure's complexity, may range from 2000 up to 6000 USD.[10,11,29,36,37] Recent studies demonstrated that application of CAD/CAM may contribute to a decrease in overall treatment costs due to shortening of operating time, possibility of immediate dental rehabilitation, and a decrease in postoperative morbidity and additional operation rates.[8-11,22,25] However, this evidence originates primarily from preliminary studies that did not infrequently analyze the effects of guides, patient-specific plates, and stereolithic models within the framework of the same experimental protocol. Thus, more evidence is needed to estimate the exact economic burden of this CAS strategy accurately.

The CAD/CAM-supported procedures also have some major limitations when it comes to the immediate reconstruction of mandibular defects after tumor resection or combat injuries. In patients with malignant neoplasms of the head and neck, the duration of the treatment should be minimized, and according to some authors, should not be longer than two weeks.[25,38] However, the total time needed to manufacture and deliver the patient-specific guides may sometimes exceed four weeks; such long idle time is associated with increased risk of tumor progression or metastasis.[10,11,25] Moreover, the originally designed VSP-specific guide may become useless if the surgical plan needs to be modified intraoperatively because wider tumor

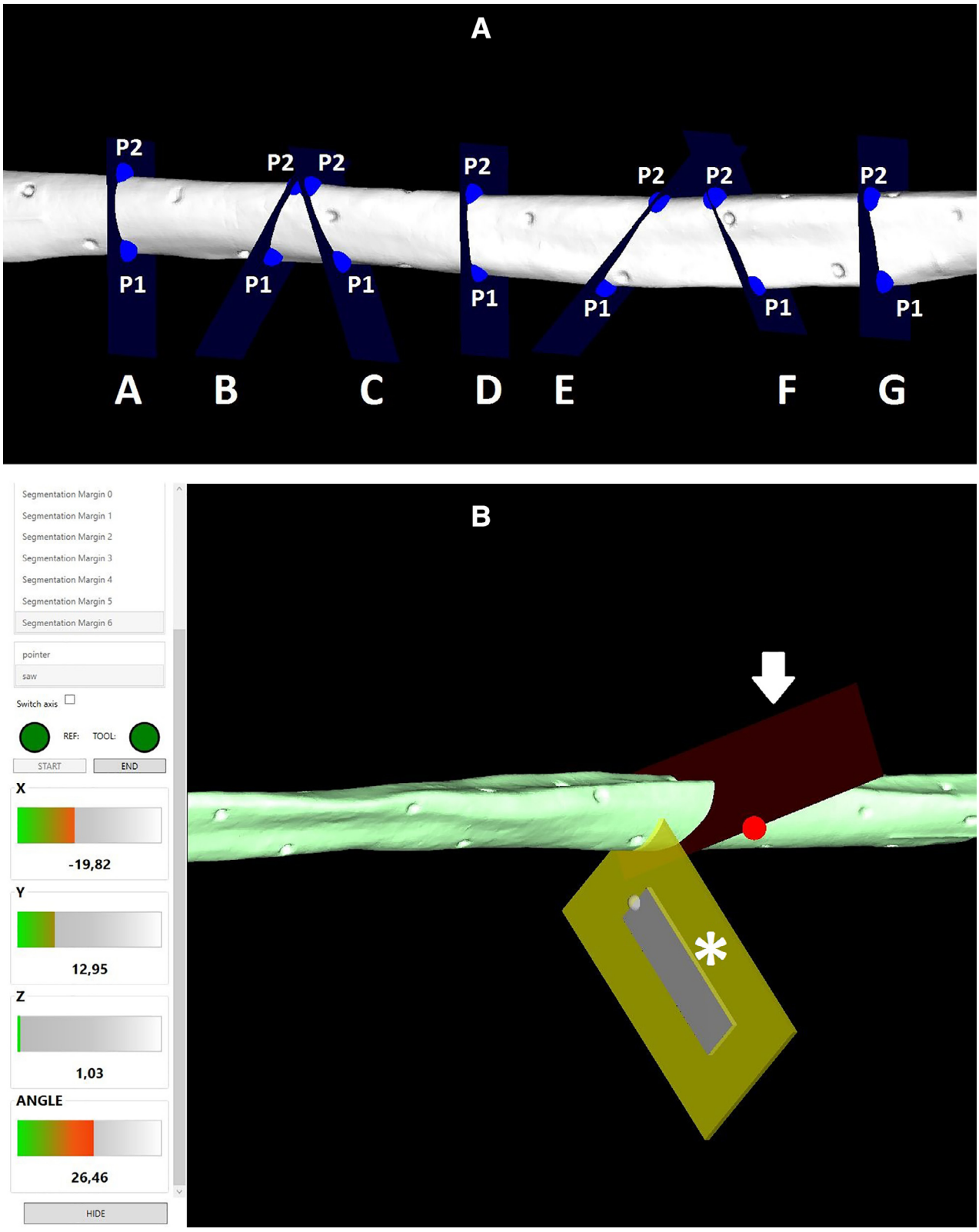

Figure 3 (A) Virtual surgery plan containing seven fibula osteotomy trajectories. For each osteotomy, a control point was set on the bone inferior (P_1) and superior edge (P_2). (B) Intraoperative screen view presenting surgical saw blade (star) navigated in accordance to virtual osteotomy plane (arrow). The bar on the left contains digital targeting information about blade position and angulation in reference to the planned cutting trajectory.

Table 1 Comparison of the registration accuracy.

Parameter		Point-pair registration			Hybrid matching registration		
		Observer A	Observer B	Summary	Observer A	Observer B	Summary
FRE	Mean ± SD (mm)	2.09 ± 0.87	1.74 ± 1.11	1.82 ± 0.96	1.43 ± 0.58	1.38 ± 0.59	1.41 ± 0.44
	Inter-observer ICC			0.699			0.927
	Intra-observer ICC	0.956	0.964	0.959	0.522	n/a	0.232
TRE	Mean ± SD (mm)	2.08 ± 0.60	1.91 ± 0.79	2.00 ± 0.67	1.45 ± 0.75	1.58 ± 0.75	1.51 ± 0.72
	Inter-observer ICC			0.674			0.861
	Intra-observer ICC	0.556	0.958	0.808	0.291	0.376	0.326

ICC, intraclass correlation coefficient.
n/a, not applicable; ICC could not be calculated due to too high intragroup variance.

Table 2 Angular deviations between the planned and actual osteotomies.

Procedure	Angular deviation Mean ± SD (°)						
	Osteotomy A	Osteotomy B	Osteotomy C	Osteotomy D	Osteotomy E	Osteotomy F	Osteotomy G
Fibula # 1	3.07 ± 0.23	2.67 ± 0.28	18.69 ± 0.35	1.72 ± 0.10	0.92 ± 0.08	8.16 ± 1.12	2.95 ± 0.54
Fibula # 2	1.81 ± 0.04	1.83 ± 0.08	15.13 ± 0.95	1.18 ± 0.59	0.56 ± 0.09	6.61 ± 1.36	0.90 ± 0.52
Fibula # 3	4.33 ± 0.02	2.73 ± 0.06	5.94 ± 0.12	3.63 ± 0.57	1.01 ± 0.14	10.01 ± 0.44	1.46 ± 0.45
Fibula # 4	3.33 ± 0.46	1.30 ± 0.10	2.63 ± 0.18	3.29 ± 0.56	1.57 ± 0.53	1.98 ± 0.47	1.64 ± 0.05
Fibula # 5	4.46 ± 0.07	4.10 ± 0.16	5.31 ± 0.18	2.59 ± 0.06	3.69 ± 0.23	5.26 ± 0.05	1.67 ± 0.11
Fibula # 6	3.41 ± 0.14	2.08 ± 0.21	1.89 ± 0.09	2.00 ± 0.14	1.33 ± 0.07	1.72 ± 0.32	3.31 ± 0.27
Summary	3.40 ± 0.93	2.45 ± 0.93	8.26 ± 6.65	2.40 ± 0.95	1.51 ± 1.08	5.62 ± 3.22	1.99 ± 0.93

Table 3 Differences between the preoperative and postoperative osteotomy control point positions.

Osteotomy control point position disparities Mean ± SD (mm)		Procedure						
		Fibula # 1	Fibula # 2	Fibula # 3	Fibula # 4	Fibula # 5	Fibula # 6	Summary
Osteotomy A	Point A	2.35 ± 0.07	1.49 ± 0.22	2.11 ± 0.14	2.69 ± 0.36	1.82 ± 0.06	2.05 ± 0.36	2.09 ± 0.43
	Point B	0.70 ± 0.38	1.31 ± 0.16	1.49 ± 0.23	3.42 ± 0.56	1.93 ± 0.08	1.86 ± 0.10	1.79 ± 0.90
Osteotomy B	Point A	1.70 ± 0.40	1.92 ± 0.23	1.96 ± 0.18	1.74 ± 0.25	1.72 ± 0.22	2.05 ± 0.37	1.85 ± 0.25
	Point B	1.93 ± 0.12	1.04 ± 0.26	1.18 ± 0.09	1.84 ± 0.04	1.05 ± 0.24	1.03 ± 0.22	1.35 ± 0.42
Osteotomy C	Point A	0.77 ± 0.04	1.79 ± 0.04	2.88 ± 0.64	3.47 ± 0.74	2.03 ± 0.23	1.47 ± 0.13	2.07 ± 0.98
	Point B	5.02 ± 0.11	5.72 ± 0.45	3.57 ± 0.33	3.99 ± 0.50	3.74 ± 0.17	1.92 ± 0.05	4.00 ± 1.27
Osteotomy D	Point A	0.80 ± 0.08	1.54 ± 0.30	0.74 ± 0.01	3.03 ± 0.26	0.83 ± 0.04	1.59 ± 0.37	1.42 ± 0.85
	Point B	1.16 ± 0.18	1.16 ± 0.16	1.61 ± 0.23	2.80 ± 0.22	1.69 ± 0.25	1.98 ± 0.47	1.74 ± 0.62
Osteotomy E	Point A	1.24 ± 0.28	1.10 ± 0.30	1.30 ± 0.37	2.19 ± 0.42	0.97 ± 0.18	0.87 ± 0.02	1.28 ± 0.50
	Point B	1.09 ± 0.16	0.80 ± 0.34	0.87 ± 0.11	2.41 ± 0.59	0.79 ± 0.04	1.16 ± 0.24	1.19 ± 0.63
Osteotomy F	Point A	1.73 ± 0.04	0.80 ± 0.08	1.91 ± 0.09	0.71 ± 0.19	1.04 ± 0.23	1.27 ± 0.17	1.25 ± 0.48
	Point B	3.61 ± 0.29	3.07 ± 0.24	2.73 ± 0.04	3.61 ± 0.12	2.81 ± 0.06	3.75 ± 0.28	3.27 ± 0.45
Osteotomy G	Point A	1.73 ± 0.37	1.09 ± 0.33	1.62 ± 0.28	0.86 ± 0.14	1.50 ± 0.02	1.65 ± 0.15	1.41 ± 0.38
	Point B	2.62 ± 0.14	0.96 ± 0.30	1.31 ± 0.37	1.58 ± 0.23	1.16 ± 0.08	1.69 ± 0.21	1.55 ± 0.59

Table 4 Tukey's post-hoc test for angular deviations between various osteotomy types.

Osteotomy	A	B	C	D	E	F	G
A		0.984	0.002	0.980	0.689	0.505	0.896
B	0.984		<0.001	1.000	0.985	0.120	1.000
C	0.002	<0.001		<0.001	<0.001	0.296	<0.001
D	0.980	1.000	<0.001		0.989	0.109	1.000
E	0.689	0.985	<0.001	0.989		0.015	1.000
F	0.505	0.120	0.296	0.989	0.015		1.000
G	0.896	1.000	<0.001	1.000	1.000	0.046	

Table 5 Advantages of intraoperative navigation over the CAD/CAM technologies.

Advantages of navigation-guided fibula free flap harvesting
Relatively low cost per procedure
Rapid implementation (even within hours)
Virtual planning that can be carried out by the surgeon
Possibility of intraoperative modification of virtual surgical plan
Capability of intraoperative identification of anatomical structures
Possibility of guided insertion of dental implants, prostheses, fixation plates and guides

resection margins are required than originally planned.[8,10,37] Although the latter limitation can be overcome by preparation of several variants of cutting templates, but this is associated with a substantial increase in the treatment cost.

Another drawback of the CAD/CAM-supported procedures stems from the fact that some guides must be ideally fitted to specific bone segments. Due to specific anatomy of the fibula, which lacks characteristic landmarks, the designed guide needs to have a large contact surface.[25,33,39] However, this drawback rarely has clinical significance and mainly concerns the cases in which guide is used along with specific prefabricated fixation plates.

Intraoperative navigation is another CAS modality that has been successfully implemented to oral and maxillofacial surgery during the last two decades. Many previous studies demonstrated the usefulness of IGS in clinical practice, inter alia in guided resections and reconstructive procedures.[27-32] Most previous studies analyzed the usefulness of intraoperative navigation during various guided implantation procedures or positioning and contouring of bone segments that have already been implanted into the mandibular region. To the best of our knowledge, the outcomes of image-guided harvesting of the FFF have been a subject of only one published study.[33] This is quite surprising considering that intraoperative navigation is in many aspects superior to widely used CAD/CAM-guided procedures, especially in the field of maxillofacial surgery (Table 5).

In this paper, we have proposed and validated a novel method of image-guided FFF harvest and fabrication. The presented algorithm enables reliable intraoperative navigation with a tip-pointer or bone cutting with a calibrated surgical saw. Although the registration process based on the skin adhesive markers only is not as precise as the hybrid registration utilizing point-pair and surface matching methods (1.82 $\pm$ 0.96 mm and 1.41 $\pm$ 0.44 mm, respectively), it still provides sufficient navigation accuracy in the fibula region (2.00 $\pm$ 0.67 mm). Moreover, this method is simple, noninvasive, and inexpensive. Therefore, it is easy to use in the routine clinical settings, which makes it superior when compared with the second registration option. Li et al. proposed mounting the reference frame in the ankle region with a belt, thus making it vulnerable to displacement and lowering navigation accuracy.[33] In our method frame is attached firmly to the anterior edge of the tibia accessed by small skin incision. Because of the tibia-fibula connections through ligaments and interosseous membrane, their positions to each other remains constant until the last phase of the operation, enabling reliable navigation with minimally invasive registration and tracking. However, to ensure tibial fixed array positional reference to the fibula, it is advisable to make each guided osteotomy incomplete until all bone cuts are made.

Results analysis showed relatively acceptable cutting trajectories' position disparity (1.85 $\pm$ 0.99 mm) and angle deviations (3.66° $\pm$ 3.60°) from the virtual plan. Overall, only one type of osteotomy exceeded 8° of deviation (osteotomy C, 8.26° $\pm$ 6.65°). However, this outcome was profoundly influenced by the first two osteotomies poor results (18.69° $\pm$ 0.35° and 15.13° $\pm$ 0.95°, respectively), probably due to the initial stage of the learning curve. The operator found both, the calibration of the sagittal saw and the blade digital targeting feature very simple to handle during the surgery. The capability of tracking saw position and angulation in reference to virtual osteotomy plane in the form of objective, digital values is a powerful addition to the standard 2D and 3D views of the virtual operative field and navigated instrument contours. It was considered particularly useful in achieving the proper angle of the cutting trajectory. It seems there might still be a possibility of improving the accuracy of the image-guided osteotomy. An important conclusion from the study is that the constant need for observation of the system screen has a negative influence on eye-hand coordination, thus lowering the precision of surgical procedure. We believe that the incorporation of the augmented reality technology would eliminate this issue, making image-guide surgery even more precise. Therefore, in the near future, we will conduct a similar study with the above-mentioned improvement to our navigation technique.

Intraoperative navigation systems are equipped with VSP software which does not require knowledge of CAD/CAM. As a result, the procedure of mandibular resection and FFF harvesting, and subsequent reconstruction of the mandible with the FFF can be planned by the surgeon, without an involvement of a CAD/CAM engineer (Figure 4). This eliminates the need for teleconferences with guide manufacturers, thus, shortening the planning process and reducing the risk of potential engineering errors.[38] As a result, the IGS can be conducted for only a few hours after obtaining CT scans, which makes this technology particularly useful for trauma and oncology surgeons. Moreover, various intraoperative scenarios, with different sizes of the resection margins, can be created. This means that the protocol of FFF harvesting can be easily amended intraoperatively whenever the extent of mandibular resection needs to be enlarged.

If the registration is correct, the navigated tool determines the location and angulation of the osteotomy

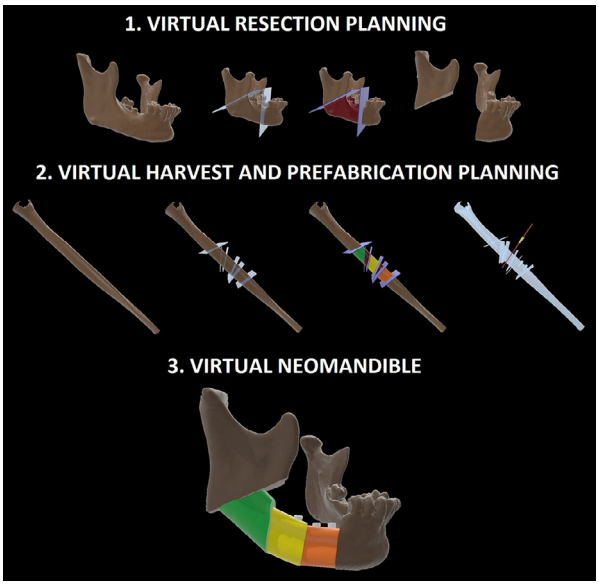

Figure 4 Summary of the complete process of virtual planning of mandible reconstruction with a free fibular flap that can be supported with the intraoperative navigation.

plane accurately. Another advantage of IGS over CAD/CAM-supported procedures is the possibility to identify anatomical structures or to verify the location of the tracked instrument in real time. However, the applicability of this function in soft tissues is limited due to structural image drift resulting from intraoperative topographic changes caused by surgical manipulation.[27-29] Nevertheless, our experiences suggest that the intraoperative navigation system is suitable for accurate localization of the key structures, such as perforator vessels and nerves, at early stages of the procedure, lowering the risk of their damage. Another application of the intraoperative navigation system is immediate insertion of osseointegrated implants to the flap's bone, which contributes to faster dental rehabilitation.[11,40]

Last but not least, the IGS procedures are considerably less costly than those involving guides. In fact, the only economic burden associated with the use of optical navigation system is the purchase of passive spheres to be mounted on the reference frame and navigated tools. The application of our system, consisting of the frame, pointer, and oscillating saw, required purchase of 10 spheres and 7 registration fiducials, with the total cost of approximately 150 USD. It needs to be emphasized that such set can be used to conduct complex mandibular resections and reconstructive surgeries. In contrast, an estimated cost of manufacturing a guide for mandibular osteotomy and another guide for FFF harvesting may exceed 4000 USD. Another argument for greater cost-effectiveness of the IGS is short duration of the osteotomy and implantation procedures and short time needed for identification of the perforator vessels. Additionally, greater accuracy of the procedure and lesser risk of intraoperative complications may contribute to lower overall treatment cost. One potential drawback of the IGS is a relatively high cost of the navigation system, starting from 50,000 USD. However, it should be remembered that the same system can be used by various specialists, e.g., neurosurgeons, orthopedists, and laryngologists, and thus, the cost of its purchase can be shared by various hospital departments.

Conclusion

The hereby-presented concept of navigated FFF modeling may become another step in the evolution of computer-assisted reconstruction of mandibular defects. Our study demonstrated that this method is suitable for accurate harvesting and fabrication of the FFF according to predefined VSP, which is not associated with a significant increase in the operating time. Moreover, the method seems to be more cost-effective than the currently popular CAD/CAM-supported procedures and may be superior to the latter in some clinical aspects, which are crucial from the perspective of maxillofacial surgery. Further studies, comparing the presented method with a cutting guide on both the simulation and cadaveric models, are needed before incorporation into clinical practice.

Acknowledgments

This work was supported by the National Centre of Research and Development of Poland, in frames of the project: "Development of Polish complementary system of molecular surgical navigation for tumor treatment" [STRATEGMED1/233624/4/NCBR/201]. The funding source had no involvement in study design, collection, analysis, and interpretation of data nor in the writing and submission of the article.

Conflict of interest

None.

Supplementary material

Supplementary material associated with this article can be found, in the online version, at doi:10.1016/j.bjps.2019.01.026.

References

1. Hidalgo PA. Fibula free flap: a new method of mandible reconstruction. *Plast Reconstr Surg* 1989;**84**:71–9.
2. Cordeiro PG, Disa JJ, Hidalgo DA, Hu QY. Reconstruction of the mandible with osseous free flaps: a 10-year experience with 150 consecutive patients. *Plast Reconstr Surg* 1999;**104**:1314–20.
3. Hidalgo DA, Pusic AL. Free-flap mandibular reconstruction: a 10-year follow-up study. *Plast Reconstr Surg* 2002;**110**:438–49.
4. Hölzle F, Kesting MR, Hölzle G, et al. Clinical outcome and patient satisfaction after mandibular reconstruction with free fibula flaps. *Int J Oral Maxillofac Surg* 2007;**36**:802–6.
5. López-Arcas JM, Arias J, Del Castillo JL, et al. The fibula osteomyocutaneous flap for mandible reconstruction: a 15-year experience. *J Oral Maxillofac Surg* 2010;**68**:2377–84.
6. Wallace CG, Chang YM, Tsai CY, Wei FC. Harnessing the potential of the free fibula osteoseptocutaneous flap in mandible reconstruction. *Plast Reconstr Surg* 2010;**125**:305–14.

7. Thankappan K, Trivedi NP, Subash P, et al. Threedimensional computed tomography-based contouring of a free fibula bone graft for mandibular reconstruction. *J Oral Maxillofac Surg* 2008;**66**:2185–92.
8. Roser SM, Ramachandra S, Blair H, et al. The accuracy of virtual surgical planning in free fibula mandibular reconstruction: comparison of planned and final results. *J Oral Maxillofac Surg* 2010;**68**:2824–32.
9. Dong Z, Li B, Xie R, Wu Q, Zhang L, Bai S. Comparative study of three kinds of fibula cutting guides in reshaping fibula for the reconstruction of mandible: an accuracy simulation study in vitro. *J Craniomaxillofac Surg* 2017;**45**:1227–35.
10. Toto JM, Chang EI, Agag R, Devarajan K, Patel SA, Topham NS. Improved operative efficiency of free fibula flap mandible reconstruction with patient-specific, computer-guided preoperative planning. *Head Neck* 2015;**37**:1660–4.
11. Avraham T, Franco P, Brecht LE, et al. Functional outcomes of virtually planned free fibula flap reconstruction of the mandible. *Plast Reconstr Surg* 2014;**134**:628–34.
12. Metzler P, Geiger EJ, Alcon A, Ma X, Steinbacher DM. Three-dimensional virtual surgery accuracy for free fibula mandibular reconstruction: planned versus actual results. *J Oral Maxillofac Surg* 2014;**72**:2601–12.
13. Chang EI, Jenkins MP, Patel SA, Topham NS. Long-term operative outcomes of preoperative computed tomography-guided virtual surgical planning for osteocutaneous free flap mandible reconstruction. *Plast Reconstr Surg* 2016;**137**:619–23.
14. Weitz J, Bauer FJ, Hapfelmeier A, Rohleder NH, Wolff KD, Kesting MR. Accuracy of mandibular reconstruction by three-dimensional guided vascularised fibular free flap after segmental mandibulectomy. *Br J Oral Maxillofac Surg* 2016;**54**:506–10.
15. Eckardt A, Swennen GR. Virtual planning of composite mandibular reconstruction with free fibula bone graft. *J Craniofac Surg* 2005;**16**:1137–40.
16. Hirsch DL, Garfein ES, Christensen AM, Weimer KA, Saddeh PB, Levine JP. Use of computeraided design and computer-aided manufacturing to produce orthognathically ideal surgical outcomes: a paradigm shift in head and neck reconstruction. *J Oral Maxillofac Surg* 2009;**67**:2115–22.
17. Antony AK, Chen WF, Kolokythas A, Weimer KA, Cohen MN. Use of virtual surgery and stereolithography-guided osteotomy for mandibular reconstruction with the free fibula. *Plast Reconstr Surg* 2011;**128**:1080–4.
18. Valentini V, Agrillo A, Battisti A, Gennaro P, Calabrese L, Iannetti G. Surgical planning in reconstruction of mandibular defect with fibula free flap: 15 patients. *J Craniofac Surg* 2005;**16**:601–7.
19. Chopra K, Manson PN, Gastman BR. Stereolithographic modeling in reconstructive surgery of the craniofacial skeleton after tumor resection. *Plast Reconstr Surg* 2012;**129**:743–5.
20. Sharaf B, Levine JP, Hirsch DL, Bastidas JA, Schiff BA, Garfein ES. Importance of computeraided design and manufacturing technology in the multidisciplinary approach to head and neck reconstruction. *J Craniofac Surg* 2010;**21**:1277–80.
21. Stirling Craig E, Yuhasz M, Shah A, et al. Simulated surgery and cutting guides enhance spatial positioning in free fibular mandibular reconstruction. *Microsurgery* 2015;**35**:29–33.
22. Lim SH, Kim YH, Kim MK, Nam W, Kang SH. Validation of a fibula graft cutting guide for mandibular reconstruction: experiment with rapid prototyping mandible model. *Comput Assist Surg* 2016;**21**:9–17.
23. Liu XJ, Gui L, Mao C, Peng X, Yu GY. Applying computer techniques in maxillofacial reconstruction using a fibula flap: a messenger and an evaluation method. *J Craniofac Surg* 2009;**20**:372–7.
24. Haddock NT, Monaco C, Weimer KA, Hirsch DL, Levine JP, Saadeh PB. Increasing bony contact and overlap with computer-designed offset cuts in free fibula mandible reconstruction. *J Craniofac Surg* 2012;**23**:1592–5.
25. Rodby KA, Turin S, Jacobs RJ, et al. Advances in oncologic head and neck reconstruction: systematic review and future considerations of virtual surgical planning and computer aided design/computer aided modeling. *J Plast Reconstr Aesthet Surg* 2014;**67**:1171–85.
26. Rohner D, Bucher P, Hammer B. Prefabricated fibular flaps for reconstruction of defects of the maxillofacial skeleton: planning, technique, and long-term experience. *Int J Oral Maxillofac Implant* 2013;**28**:221–9.
27. Schramm A, Gellrich NC, Gutwald R, et al. Indications for computer-assisted treatment of cranio-maxillofacial tumors. *Comput Aided Surg* 2000;**5**:343–52.
28. Feichtinger M, Pau M, Zemann W, Aigner RM, Karcher H. Intraoperative control of resection margins in advanced head and neck cancer using a 3D-navigation system based on PET/CT image fusion. *J Craniomaxillofac Surg* 2010;**38**:589–594.
29. Pietruski P, Majak M, Swiatek-Najwer E, et al. Accuracy of experimental mandibular osteotomy using the image-guided sagittal saw. *Int J Oral Maxillofac Surg* 2016;**45**:793–800.
30. Wu J, Sun J, Shen SG, Xu B, Li J, Zhang S. Computer-assisted navigation: its role in intraoperatively accurate mandibular reconstruction. *Oral Surg Oral Med Oral Pathol Oral Radiol* 2016;**122**:134–42.
31. Gui H, Yang H, Shen SG, Xu B, Zhang S, Bautista JS. Image-guided surgical navigation for removal of foreign bodies in the deep maxillofacial region. *J Oral Maxillofac Surg* 2013;**71**:1563–71.
32. Ewers R, Schicho K, Truppe M, et al. Computer aided navigation in dental implantology: 7 years of clinical experience. *J Oral Maxillofac Surg* 2004;**62**:329–34.
33. Li P, Xuan M, Liao C, et al. Application of intraoperative navigation for the reconstruction of mandibular defects with microvascular fibular flaps-preliminary clinical experiences. *J Craniofac Surg* 2016;**27**:751–5.
34. Świątek-Najwer E, Żuk M, Majak M, Popek M. The rigid registration of CT and scanner dataset for computer aided surgery. In: *Proceedings of the VI ECCOMAS thematic conference on computational vision and medical image processing, VipIMAGE*, 27; 2017. p. 345–53.
35. Fitzpatrick JM, West JB. The distribution of target registration error in rigid-body point-based registration. *IEEE Trans Med Imaging* 2001;**20**:917–27.
36. Rustemeyer J, Melenberg A, Sari-Rieger A. Costs incurred by applying computer-aided design/computer-aided manufacturing techniques for the reconstruction of maxillofacial defects. *J Craniomaxillofac Surg* 2014;**42**:2049–55.
37. Pietruski P, Majak M, Świątek-Najwer E, et al. Image-guided bone resection as a prospective alternative to cutting templates – a preliminary study. *J Craniomaxillofac Surg* 2015;**43**:1021–7.
38. Mazzoni S, Marchetti C, Sgarzani R, Cipriani R, Scotti R, Ciocca L. Prosthetically guided maxillofacial surgery: evaluation of the accuracy of a surgical guide and custom-made bone plate in oncology patients after mandibular reconstruction. *Plast Reconstr Surg* 2013;**131**:1376–85.
39. Zhao L, Patel PK, Cohen M. Application of virtual surgical planning with computer assisted design and manufacturing technology to cranio-maxillofacial surgery. *Arch Plast Surg* 2012;**39**:309–16.
40. Wei FC, Santamaria E, Chang YM, Chen HC. Mandibular reconstruction with fibular osteoseptocutaneous free flap and simultaneous placement of osseointegrated dental implants. *J Craniofac Surg* 1997;**8**:512–21.